

Fig. 4. Observation of immunological synapse formation inside a LN. SNARF-labeled (red) naïve CD43-GFP⁺ T cells (13) were injected intravenously into mice given DiD-labeled antigen-pulsed DCs 12 hours before. Popliteal LNs were imaged 23 hours later by acquiring a series of z sections throughout the contact region. **(A)** One section through the equatorial plane of the synapse shows exclusion of the green signal coming from the CD43-GFP. **(B)** The en face view shows that this pattern of exclusion is quite broad with a peripheral ring of CD43 surrounding a central region labeled with the cytoplasmic red dye. **(C)** A three-dimensional representation of the merged sections shows that the two T cells bound to this DC both exclude CD43 from the zone of membrane contact (synapse).

hematopoietic cell interactions in architecturally intact lymphoid tissue will open an even more complete window on the events involved in antigen-specific immune reactions.

References and Notes

1. E. C. Butcher, M. Williams, K. Youngman, L. Rott, M. Briskin, *Adv. Immunol.* **72**, 209 (1999).
2. I. Mellman, R. M. Steinman, *Cell* **106**, 255 (2001).
3. C. Reis e Sousa, *Immunity* **14**, 495 (2001).
4. J. G. Cyster, *Science* **286**, 2098 (1999).
5. M. K. Jenkins et al., *Annu. Rev. Immunol.* **19**, 23 (2001).
6. P. Garside et al., *Science* **281**, 96 (1998).
7. C. R. Monks, B. A. Freiberg, H. Kupfer, N. Sciaky, A. Kupfer, *Nature* **395**, 82 (1998).
8. J. Delon, N. Bercovici, G. Raposo, R. Liblau, A. Trautmann, *J. Exp. Med.* **188**, 1473 (1998).
9. A. Grakoui et al., *Science* **285**, 221 (1999).
10. M. Gunzer et al., *Immunity* **13**, 323 (2000).
11. M. F. Krummel, M. D. Sjaastad, C. Wülfing, M. M. Davis, *Science* **289**, 1349 (2000).
12. E. Ingulli, A. Mondino, A. Khoruts, M. K. Jenkins, *J. Exp. Med.* **185**, 2133 (1997).
13. Supporting online material is available on Science Online at www.sciencemag.org/cgi/content/full/296/5574/1873/DC1.
14. M. L. Dustin, S. K. Bromley, Z. Kan, D. A. Peterson, E. R. Unanue, *Proc. Natl. Acad. Sci. U.S.A.* **94**, 3909 (1997).
15. J. Sprent, J. F. Miller, G. F. Mitchell, *Cell. Immunol.* **2**, 171 (1971).
16. C. Tanchot, D. L. Barber, L. Chiodetti, R. H. Schwartz, *J. Immunol.* **167**, 2030 (2001).
17. J. Delon, K. Kaibuchi, R. N. Germain, *Immunity* **15**, 691 (2001).
18. G. A. Hollander, B. D. Luskey, D. A. Williams, S. J. Burakoff, *J. Immunol.* **149**, 438 (1992).
19. S. Stoll, unpublished observations.
20. P. Reichert, R. L. Reinhardt, E. Ingulli, M. K. Jenkins, *J. Immunol.* **166**, 4278 (2001).
21. C. C. Caldwell et al., *J. Immunol.* **167**, 6140 (2001).
22. S. Valitutti, S. Muller, M. Dessing, A. Lanzavecchia, *Eur. J. Immunol.* **26**, 2012 (1996).
23. J. Banchemareau, R. M. Steinman, *Nature* **392**, 245 (1998).
24. C. Reis e Sousa, A. Sher, P. Kaye, *Curr. Opin. Immunol.* **11**, 392 (1999).
25. J. Delon, R. N. Germain, *Curr. Biol.* **10**, R923 (2000).
26. R. N. Germain, *Science* **293**, 240 (2001).
27. P. E. Lipsky, A. S. Rosenthal, *J. Exp. Med.* **141**, 138 (1975).
28. J. M. Serrador et al., *Blood* **91**, 4632 (1998).
29. P. T. So, C. Y. Dong, B. R. Masters, K. M. Berland, *Annu. Rev. Biomed. Eng.* **2**, 399 (2000).
30. We thank O. Schwartz (National Institute of Allergy and Infectious Diseases confocal facility) for help with the acquisition of images. Supported by postdoctoral fellowships from the Deutsche Forschungsgemeinschaft (S.S.) and the Human Frontier Science Program (J.D.).

20 February 2002; accepted 25 April 2002

Dynamics of Thymocyte–Stromal Cell Interactions Visualized by Two-Photon Microscopy

Philippe Bousso,¹ Nirav R. Bhakta,^{2*} Richard S. Lewis,² Ellen Robey^{1†}

Thymocytes are selected to mature according to their ability to interact with self major histocompatibility complex (MHC)–peptide complexes displayed on the thymic stroma. Using two-photon microscopy, we performed real-time analysis of the cellular contacts made by developing thymocytes undergoing positive selection in a three-dimensional thymic organ culture. A large fraction of thymocytes within these cultures were highly motile. MHC recognition was found to increase the duration of thymocyte–stromal cell interactions and occurred as both long-lived cellular associations displaying stable cell–cell contacts and as shorter, highly dynamic contacts. Our results identify the diversity and dynamics of thymocyte interactions during positive selection.

Tissue microenvironments are likely to have a profound impact on lymphocyte behavior, yet most studies of lymphocytes have relied on monolayer cultures or fixed-tissue preparations that fail to recapitulate the complexity and the dynamics of cellular environments. With respect to T cell development, fundamental questions remain about how thymo-

cytes behave within the three-dimensional stromal cell network required for their differentiation. Generation of an efficient repertoire of mature $\alpha\beta$ T lymphocytes by positive selection is governed by interactions between the T cell antigen receptor (TCR) of immature CD4⁺CD8⁺ double-positive (DP) thymocytes and the array of self MHC–peptide complexes displayed on the surface of thymic stromal cells (1–3). The patterns of thymocyte motility during this process, the dynamics and the topology of thymocyte–stromal cell interactions, and the influence of MHC recognition on these cellular contacts have yet to be characterized.

The advent of two-photon laser scanning microscopy (TPLSM) offers a powerful

¹Department of Molecular and Cell Biology, University of California, Berkeley, CA 94720, USA. ²Department of Molecular and Cellular Physiology, Stanford University School of Medicine, Stanford, CA 94305, USA.

*This author made independent, essential contributions to this work.

†To whom correspondence should be addressed. E-mail: erobey@uclink4.berkeley.edu

REPORTS

method for addressing these questions. TPLSM provides the ability to track fluorescently labeled cells over time deep within light-scattering tissue, while largely avoiding the problems of bleaching and phototoxicity associated with conventional confocal microscopy (4). We used TPLSM in conjunction with the well-characterized reaggregate thymic organ culture (RTOC) system (5, 6) to study the dynamics of thymocyte–thymic stromal cell interactions in a three-dimen-

sional tissue environment relevant for thymocyte development (7).

The F5 TCR recognizes an influenza peptide presented by class I MHC-D^b, and F5 TCR transgenic mice on the C57BL/6 (H-2^b) background display strong positive selection of CD8 single-positive (SP) T cells (8). We used thymocytes from F5 TCR β_2 -microglobulin^{-/-} mice (hereafter referred to as F5 thymocytes) as a source of preselection thymocytes. F5 thymocytes differentiated into

CD8 SP cells when cocultured as a reaggregate with thymic stromal cells derived from C57BL/6 (referred to as wild-type) mice (fig. S1) (9). F5 CD8 SP generated in this organotypic culture system displayed the hallmarks of mature T cells, including high levels of TCR expression, and have been shown to be functionally competent (9). No mature SP thymocytes developed when F5 thymocytes were reaggregated with stromal cells derived from MHC^{-/-} fetal thymic lobes (fig. S1).

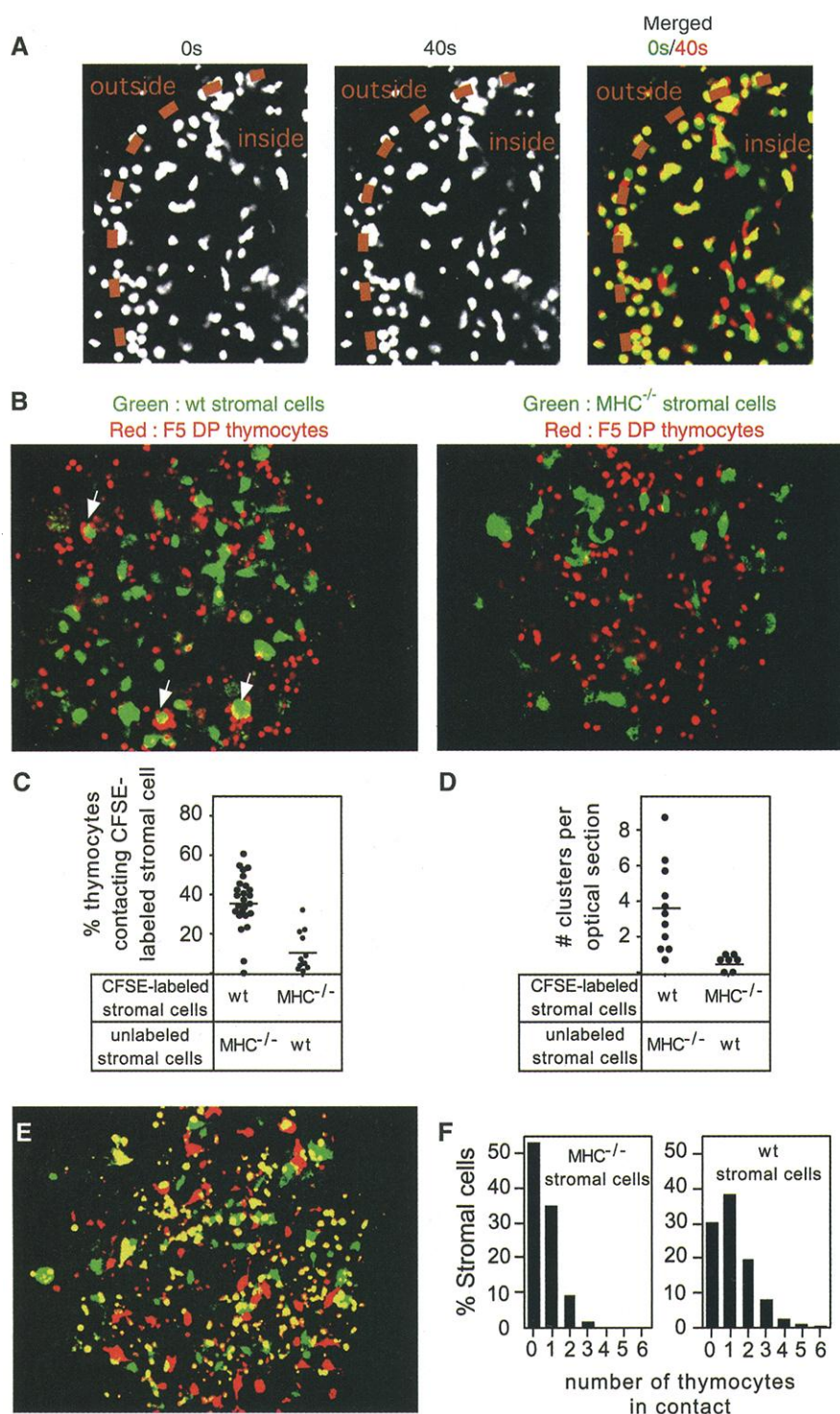


Fig. 1. MHC recognition increases the duration of thymocyte–thymic stromal cell interactions. **(A)** Active crawling of thymocytes located inside reaggregate organ cultures. Two TPLSM images of the same RTOC are shown, imaged 40 s apart. Dashed line indicates the limit of the tissue. In the merged image of the two time points (right panel), nonmotile thymocytes appear yellow (because of the overlap of green and red images), whereas motile thymocytes appear as green-red doublets. Note that virtually all thymocytes at the surface of the lobe are rounded and nonmotile. By contrast, a large fraction of thymocytes located inside the tissue display an elongated shape and are highly motile. **(B)** Preferential association of F5 DP thymocytes with MHC-bearing stromal cells. Left panel: Representative optical section of an RTOC lobe containing F5 DP thymocytes (red) together with 95% unlabeled MHC^{-/-} thymic stromal cells and 5% CFSE-labeled wild-type thymic stromal cells (green). Note that a large fraction of F5 DP cells selectively contact wild-type stromal cells, resulting in the formation of clusters (arrows). Right panel: Representative optical section of a control lobe containing F5 DP thymocytes (red) together with 95% unlabeled wild-type thymic stromal cells and 5% CFSE-labeled MHC^{-/-} thymic stromal cells (green). **(C and D)** For each individual lobe containing the indicated stromal cell mixture, the percentage of F5 DP thymocytes contacting a labeled thymic stromal cell **(C)** and the number of clusters per optical section **(D)** were quantified by an unbiased observer (7). Differences between the two groups were statistically significant: $P < 0.00001$ and $P < 0.01$ for **(C)** and **(D)**, respectively. **(E)** Representative optical section of a lobe containing F5 DP thymocytes double-labeled with SNARF and CFSE (yellow) together with 90% unlabeled MHC^{-/-} stromal cells, 5% SNARF-labeled MHC^{-/-} (red), and 5% CFSE-labeled wild-type (wt) stromal cells (green). **(F)** Lobes were formed as in **(E)** and the number of F5 DP thymocytes contacting each individual MHC^{-/-} or wild-type stromal cell was recorded. Percentage of MHC^{-/-} (left) or wild-type (right) stromal cells contacting the indicated number of thymocytes is shown. Wild-type stromal cells have on average 1.17 thymocytes in contact, whereas MHC^{-/-} stromal cells have on average 0.57 thymocyte in contact. Results were obtained by analyzing 180 MHC^{-/-} and 289 wild-type thymic stromal cells. Differences between frequency distributions were statistically significant ($P < 0.001$, χ^2 test).

REPORTS

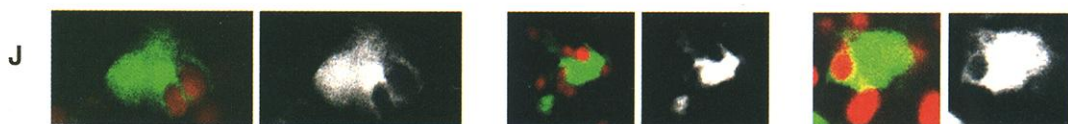
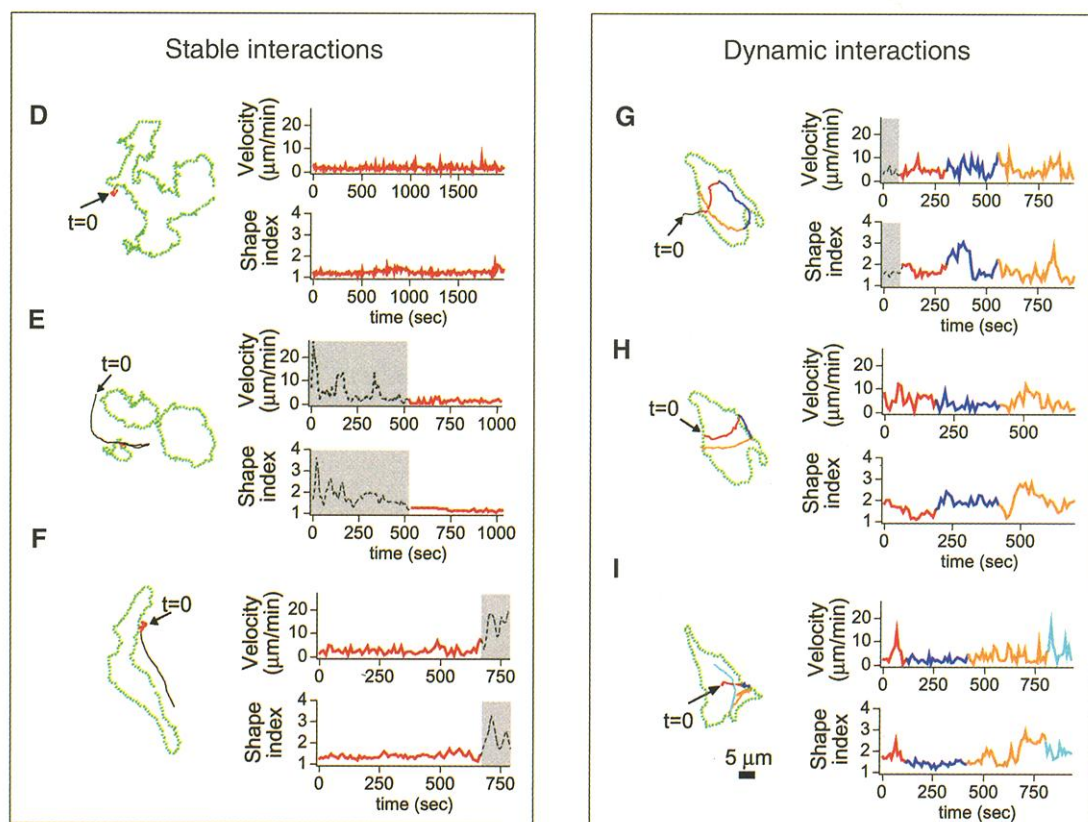
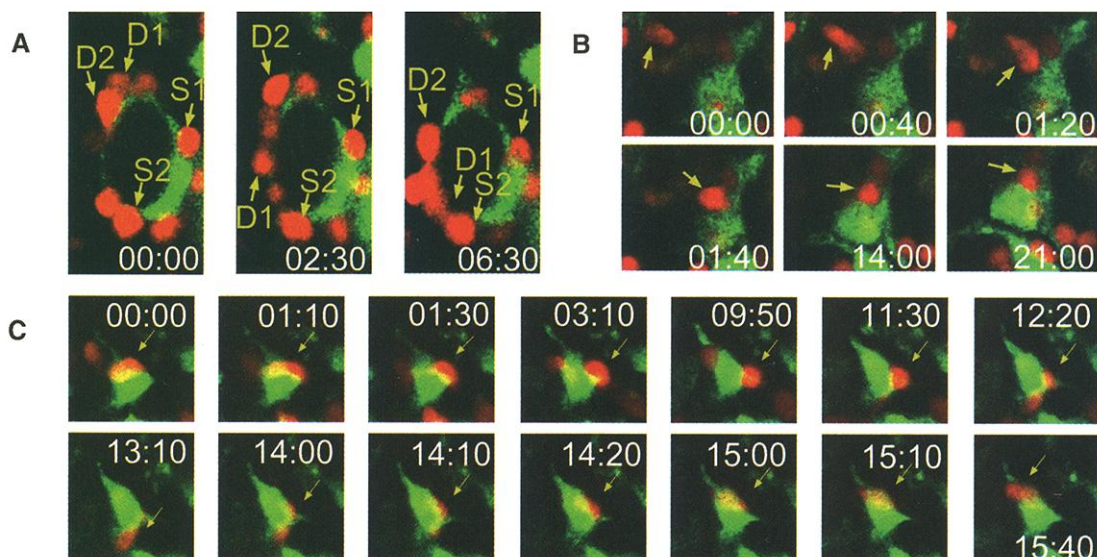
To assess whether developing thymocytes located within the organ culture could be detected by two-photon microscopy, we pu-

rified F5 CD4⁺CD8⁺ (F5 DP) cells and labeled them with the vital dye SNARF (7); then we reaggregated them with wild-type

stromal cells. With TPLSM imaging, individual thymocytes located inside the tissue could be detected up to 100 μm below the tissue

Fig. 2. MHC recognition can

result in both stable and dynamic cell-cell contacts. RTOCs were formed with F5 DP thymocytes (red), wild-type thymic stromal cells (green), and excess unlabeled MHC^{-/-} stromal cells and cultured for 16 to 20 hours. Data were collected ~ 40 μm below the tissue surface. Time-lapse movies of these and other interactions are available in movies S3 to S11. The time in minutes and seconds is indicated for each frame. (A) Stable and dynamic contacts are associated with the same stromal cell. Individual thymocytes S1 and S2 (stable contacts) and D1 and D2 (dynamic contacts) are shown. (B) Example of a stable association in which the thymocyte makes contact with a wild-type stromal cell and stops crawling. (C) Example of a dynamic association in which the thymocyte is actively crawling while it remains attached to the thymic stromal cell. (D to I) Quantitation of velocity and cell-shape changes of thymocytes engaged in stable (D to F) or dynamic (G to I) interactions. A shape index close to 1 indicates a rounded shape, whereas higher values reflect cell elongation (7). Dashed lines and shaded areas correspond to time points when the thymocyte is not contacting the stromal cell. To the left of each set of plots is a trace of the thymocyte trajectory, with stromal cells indicated in green. Different colors indicate the relationship between the cell trajectory and the corresponding velocity and cell-shape plots. (D) Example of an association that remains stable for the entire period of imaging (typical of >90% of the observed stable associations). (E) Stable association in which we recorded the initial encounter with the stromal cell (movie S5). (F) Stable association in which we recorded the detachment from the stromal cell (movie S8). (G to I) Examples of dynamic contacts. Two thymocytes interacting with the same stromal cell are shown in (G) and (H) (movie S11). Thymocytes engaged in dynamic contacts with stromal cells exhibit fluctuations in velocity and shape that generally correspond to changes in direction as the thymocyte crawls across the



stromal cell. (J) Examples of partial enclosure of thymocytes by thymic stromal cells. Merged images are displayed next to the fluorescent signals from the stromal cells. Note gaps in the stromal cell signal corresponding to the location of the thymocyte.

stromal cell. (J) Examples of partial enclosure of thymocytes by thymic stromal cells. Merged images are displayed next to the fluorescent signals from the stromal cells. Note gaps in the stromal cell signal corresponding to the location of the thymocyte.

REPORTS

surface (fig. S2). Because RTOCs in these experiments are $\sim 200 \mu\text{m}$ across, it was possible to image virtually any labeled cell in the organ culture.

With time-lapse imaging, we observed a significant fraction of F5 DP thymocytes (ranging from 10% to 50%) migrate vigorously in the organ culture. We observed both motile and nonmotile thymocytes regardless of whether the thymocytes expressed selectable TCRs (10). Active crawling of thymocytes was not restricted to the RTOC system, because green fluorescent protein-expressing DP thymocytes in an intact, reseeded fetal thymic lobe displayed similar behavior (movie S1). Active cell motility appeared to be most highly favored when thymocytes were surrounded completely by the network of stromal cells. Although virtually all thymocytes situated at the surface of the RTOC lobe were rounded and sessile, many thymocytes located within the lobe displayed an elongated shape and an active crawling motion (Fig. 1A) (movie S2).

The observation that thymocytes in thymic organ culture can be highly motile raises the question of whether MHC recognition by thymocytes involves prolonged associations with stromal cells. Indeed, mature T cell-antigen-presenting cell (APC) interactions are not prolonged by the presence of antigen under conditions that favor T cell crawling (11). On the other hand, T cells were found to form clusters with antigen-pulsed APCs *in vivo* (12). To assess whether MHC recognition during positive selection influences the duration of thymocyte-thymic stromal cell interactions, we prepared RTOCs with SNARF-labeled F5 DP thymocytes with a limited number of carboxyfluorescein diacetate succinimidyl ester (CFSE)-labeled thymic stromal cells (wild-type) capable of promoting selection and an excess of unlabeled nonselecting (MHC^{-/-}) stromal cells. Because only the labeled stromal cells could provide the signals required for positive selection, we

reasoned that if MHC recognition substantially increases the duration of thymocyte-thymic stromal cell interactions, F5 DP thymocytes should preferentially contact MHC-bearing stromal cells. After 16 to 20 hours of culture, we observed a large fraction of F5 thymocytes ($36\% \pm 2.8\%$; mean \pm SEM; $n = 25$) to be in contact with MHC-bearing stromal cells (Fig. 1, B and C), which often resulted in the formation of clusters around individual wild-type stromal cells (3.7 ± 0.7 clusters per optical section, mean \pm SEM; Fig. 1D). In contrast, we observed virtually no clusters (0.6 ± 0.2 cluster per optical section) and few thymocytes ($11\% \pm 2.9\%$; $n = 12$) in contact with CFSE-labeled stromal cells in control lobes made with excess unlabeled wild-type stromal cells and a limited number of CFSE-labeled MHC^{-/-} stromal cells (Fig. 1, B to D).

To extend these observations, we compared the propensity of individual MHC^{-/-} and wild-type thymic stromal cells to interact with F5 DP cells in the same lobe. For this purpose, we double-labeled F5 DP thymocytes with SNARF and CFSE (which appear yellow in merged fluorescence images) and reaggregated them with 90% unlabeled MHC^{-/-} stromal cells, 5% SNARF-labeled MHC^{-/-} stromal cells, and 5% CFSE-labeled wild-type stromal cells. We then measured the number of thymocytes in contact with each individual labeled stromal cell (MHC^{-/-} or wild type). Most wild-type stromal cells (70%) interacted with at least one F5 DP cell, whereas only 47% of MHC^{-/-} stromal cells were contacting any thymocytes (Fig. 1, E and F). These results confirm the preferential association of F5 thymocytes with positively selecting stromal cells and indicate that these interactions are not restricted to a minor subpopulation of thymic stromal cells.

The preferential association between F5 TCR thymocytes and wild-type stromal cells in RTOC containing excess MHC^{-/-} stromal cells implies that most of the cellular contacts made by F5 thymocytes with wild-type stro-

mal cells in these cultures were driven by MHC recognition. Therefore, we analyzed the dynamics of these interactions in this system by imaging individual cell-cell contacts over time. We identified two distinct patterns of contact and categorized them as stable or dynamic on the basis of whether the F5 thymocyte contacting the wild-type stromal cell was nonmotile (stable) or was actively crawling (dynamic) along the stromal cell (Fig. 2). We could observe both types of interactions in the same optical section of a given lobe (fig. S3A) and even associated with the same stromal cell (Fig. 2A) (movie S3).

We observed the first type of interactions, characterized by a very stable cell-cell contact, in 54% of the cases (93/172). In nearly all of the interactions in this group ($\sim 95\%$), the contact was maintained during the entire 30-min observation period (Fig. 2D) (movie S4). These stable interactions were characterized by a rounded and unchanging thymocyte morphology (Fig. 2, D to F). In several instances, we recorded the initial cell encounter during the time of imaging. In all these cases, the migrating thymocyte stopped within seconds of encounter with the MHC-bearing stromal cell and remained attached for the remainder of the imaging period (Fig. 2, B and E) (fig. S3B; movies S5 and S6). Detachment was a rare event (3 to 6 times in >35 hours of cumulative observation); in the few observed cases, it resulted in reacquisition of a migratory behavior (Fig. 2F) (fig. S3C; movies S7 and S8). Based on the low frequency of detachment, we estimated the mean duration of these interactions to be in the range of 6 to 12 hours (Table 1) (7).

The second type of interactions, encompassing 46% of the cellular associations, was characterized by highly dynamic cell-cell contacts (Fig. 2, C and G to I) (fig. S3D; movies S9 to S11). In these cases, F5 DP thymocytes were highly motile while maintaining contact with the stromal cell. Thymocytes engaged in dynamic contacts displayed fluctuations in their velocities and cell shapes that often correlated with changes in direction as they crawled along the surface of a stromal cell (Fig. 2, G to I). The estimated mean duration of the dynamic interactions was substantially shorter than that of the stable group (13 to 36 min; Table 1). The presence of dynamic interactions between thymocytes and MHC^{+/+} stroma raises the possibility that TCR recognition is not necessarily associated with a stop signal.

In 16% of stable interactions and 11% of dynamic interactions, the thymocyte appeared to be partly enclosed within the stromal cell (Table 1 and Fig. 2J) (fig. S3E). Partly enclosed thymocytes appeared to be viable and, in some cases, remained motile during and after enclosure (movie S10). These observations are rem-

Table 1. Types of thymocyte-stromal cell interactions observed in a model of positive selection (7). We examined 172 individual thymocyte-stromal cell contacts from nine individual RTOCs containing labeled F5 DP thymocytes, a limited number of labeled wild-type stromal cells, and an excess of MHC^{-/-} stromal cells (Fig. 1B). Data were taken from time-lapse images of the same optical section taken every 10 s for ~ 30 min (typically $40 \mu\text{m}$ beneath the tissue surface). All cell interactions for which the contact could be observed for at least 200 s are included in this analysis. We categorized these contacts as stable or dynamic on the basis of whether the thymocyte was nonmotile (stable) or was actively crawling along the stromal cell (dynamic). Representative examples are shown in Fig. 2 and in movies S3 to S11.

	Stable cell-cell contact	Dynamic cell-cell contact
Observed interactions	93/172 (54.0%)	79/172 (46.0%)
Interactions with thymocyte enclosure	15/93 (16%)	9/79 (11%)
Accumulated time of imaging	35 hours 30 min	10 hours 27 min
Observed detachment events	3 to 6	17 to 29
Estimated mean duration of interaction (7)	6 to 12 hours	13 to 36 min

incent of previous reports suggesting thymocyte enclosure by thymic epithelial cells (13, 14). This unique cellular topology might play a role in some aspect of thymic selection, perhaps serving to increase the surface area of the association.

In our system, there was a >3-fold increase in the proportion of thymocytes contacting wild-type versus MHC^{-/-} stromal cells (Fig. 1C); this finding implies that most of the described interactions depended on MHC recognition. In addition, we observed multiple stable and dynamic contacts within large clusters of thymocytes (Fig. 2) (movie S3) and these structures were formed only around MHC-bearing stromal cells (Fig. 1D). Thus, although a small fraction of the described interactions may have been MHC independent, a substantial proportion of both stable of dynamic contacts observed in our system were associated with MHC recognition. Future experiments with molecular markers of TCR signaling are needed to directly identify individual MHC-driven interactions.

This study documents the cellular interactions between thymocytes and stromal cells during positive selection within a three-dimensional tissue environment. Mature T cell activation can result from a stable, long-lasting interaction with an APC (15, 16) but may also result from summing of multiple transient encounters with APCs (11, 17). Our observation that MHC recognition by thymocytes is associated with both stable and dynamic contacts with thymic stromal cells raises the possibility that both modes of TCR signaling may occur during positive selection. The basis for the observed diversity of thymocyte–thymic stromal cell interactions is unclear. One possibility is that these different patterns of interaction involve distinct types of stromal cells. This is unlikely to be the sole explanation, because both stable and dynamic contacts have been repeatedly observed at the surface of the same stromal cell (Fig. 2A) (movies S3 and S10). Alternatively, the different interaction patterns could be associated with different signals or could correspond to different stages of positive selection. Following the history of TCR signals received by an individual thymocyte during the whole process of thymocyte maturation remains challenging but ultimately should help to answer these questions. More generally, the use of TPLSM to track the fate of immune cells within lymphoid tissues should provide new insights into lymphocyte biology and development.

References and Notes

1. L. J. Berg, J. Kang, *Curr. Opin. Immunol.* **13**, 232 (2001).
 2. K. A. Hogquist, *Curr. Opin. Immunol.* **13**, 225 (2001).
 3. P. Marrack, J. Kappler, *Curr. Opin. Immunol.* **9**, 250 (1997).
 4. W. Denk, J. H. Strickler, W. W. Webb, *Science* **248**, 73 (1990).

5. E. J. Jenkinson, G. Anderson, J. J. Owen, *J. Exp. Med.* **176**, 845 (1992).
 6. G. Anderson, J. J. Owen, N. C. Moore, E. J. Jenkinson, *J. Immunol.* **153**, 1915 (1994).
 7. Supplementary material is available on Science Online.
 8. C. Mamalaki et al., *Dev. Immunol.* **3**, 159 (1993).
 9. Y. Tanaka et al., *Int. Immunol.* **9**, 381 (1997).
 10. P. Bousso, unpublished data.
 11. M. Gunzer et al., *Immunity* **13**, 323 (2000).
 12. E. Ingulli, A. Mondino, A. Khoruts, M. K. Jenkins, *J. Exp. Med.* **185**, 2133 (1997).
 13. R. Brelinska, J. B. Warchol, *Microsc. Res. Tech.* **38**, 250 (1997).
 14. M. Pezzano, M. Samms, M. Martinez, J. Guyden, *Microbiol. Mol. Biol. Rev.* **65**, 390 (2001).
 15. C. R. Monks, B. A. Freiberg, H. Kupfer, N. Sciaky, A. Kupfer, *Nature* **395**, 82 (1998).
 16. A. Grakoui et al., *Science* **285**, 221 (1999).

17. D. M. Underhill, M. Bassetti, A. Rudensky, A. Aderem, *J. Exp. Med.* **190**, 1909 (1999).
 18. We thank B. J. Fowlkes, D. Raullet, and members of the Robey laboratory for critical reading of the manuscript; J. Owen for advice on preparing RTOC cultures; and S. Smith and N. O'Rourke for help in designing and constructing the two-photon microscope. Supported by NIH grants AI32985 and AI42033 (E.R.) and GM45374 (R.S.L.). P.B. is supported by the Cancer Research Institute. N.R.B. is supported by the Medical Scientist Training Program at Stanford.

Supplementary Online Material

www.sciencemag.org/cgi/content/full/296/5574/1876/DC1
 Figs. S1 to S3
 Movies S1 to S11

15 February 2002; accepted 25 April 2002

Activation of Endothelial Cell Protease Activated Receptor 1 by the Protein C Pathway

Matthias Riewald,¹ Ramona J. Petrovan,¹ Aaron Donner,¹ Barbara M. Mueller,² Wolfram Ruf^{1*}

The coagulant and inflammatory exacerbation in sepsis is counterbalanced by the protective protein C (PC) pathway. Activated PC (APC) was shown to use the endothelial cell PC receptor (EPCR) as a coreceptor for cleavage of protease activated receptor 1 (PAR1) on endothelial cells. Gene profiling demonstrated that PAR1 signaling could account for all APC-induced protective genes, including the immunomodulatory monocyte chemoattractant protein-1 (MCP-1), which was selectively induced by activation of PAR1, but not PAR2. Thus, the prototypical thrombin receptor is the target for EPCR-dependent APC signaling, suggesting a role for this receptor cascade in protection from sepsis.

Tissue factor–initiated coagulation in sepsis triggers a lethal response (1–3) that may involve coagulation protease–mediated proinflammatory signaling through heterotrimeric GTP-binding protein (G-protein)–coupled protease-activated receptors (PARs) (4–7). The PC pathway protects animals from *Escherichia coli*–induced lethality (8–10) and APC reduces mortality in patients with severe sepsis (11). PC bound to EPCR is activated by a coagulation feedback loop in which traces of thrombin, once bound to thrombomodulin, specifically activate PC (12). APC is a trypsin-like coagulation protease and PARs serve as the cellular sensors for these enzymes (4, 5). The PC anticoagulant pathway operates on endothelial cells that express PAR1 and PAR2 along with EPCR. Proteolytic signaling by APC induces protective

responses in endothelial cells (13), but the involvement of PARs in this process remains unclear.

PAR1-deficient murine fibroblasts are not activated by proteases unless transfected with an appropriate PAR (6, 7). We exploited the unresponsiveness of these cells to APC to characterize the requirement for protease signaling by APC (14). Stimulation with APC was performed in the presence of 100 nM hirudin, which blocks all cell-surface thrombin-mediated PAR1 signaling (15). PAR1-deficient fibroblasts were responsive to 20 nM APC only when EPCR was coexpressed with a PAR (Fig. 1A). Expression of EPCR or PAR2 alone or coexpression of PAR2 with an EPCR mutant (EPCR A154) deficient in APC binding (16) failed to support APC signaling. These results show that only EPCR-bound APC can efficiently activate PARs.

Coexpression of EPCR and PAR1 also resulted in responsiveness to APC (Fig. 1B). Like thrombin signaling, APC signaling was inhibited by PAR1 cleavage–blocking antibodies, whereas antibodies to PAR1 did not prevent signaling by the

¹Department of Immunology, C204, The Scripps Research Institute, 10550 North Torrey Pines Road, La Jolla, CA 92037, USA. ²Division of Cancer Biology, La Jolla Institute for Molecular Medicine, 4570 Executive Drive, San Diego, CA 92121, USA.

*To whom correspondence should be addressed. E-mail: ruf@scripps.edu